



Comparison of the ultra-filtration and cation exchange membrane performance in photo electro catalytic degradation of methylene blue

Seyed Ali Rahmaninezhad, Nasser Mehrdadi, Zaynab Mahzari

Environmental Engineering Department, University of Tehran, Tehran, Iran.

Received 9 Sep. 2019; Received in revised form 2 Oct. 2019; Accepted 14 Oct. 2019; Available online 1 Nov. 2019

Abstract

Energy gathering from hardly biodegradable and toxic industrial wastewaters, especially textile disposals during their treatment is a promising achievement that could be provided by advanced oxidation methods, like Photo-Electro-Catalysis (PEC). The current density and efficiency of organic removal as dependent parameters can be influenced by the type of anode and cathode separating membrane. In this study, the performance of PEC on Methylene Blue (MB) as an organic material and produced power is evaluated by comparing Ultra-Filtration (UF) and Cation Exchange Membranes (CEM). The results show that in the case of CEM, the removal percent of MB in anolyte is more than that of UF membrane, while the produced power between anode and cathode electrodes are more in UF case. Moreover, the increase in electric conductivity of catholyte has a direct relation to the performance of PEC both in UF and CEM case, while it is more effective in UF case. Also, the investigation of six applied kinetics models reveals the MB concentration of anolyte photodegradation in case of CEM has higher order of magnitude rather than UF case.

Copyright © 2019 International Energy and Environment Foundation - All rights reserved.

Keywords: Advanced oxidation method; Photo-Electro-Catalysis; Ultra-filtration membrane; Cation exchange membranes; Kinetics model.

1. Introduction

Providing energy to treat wastewater is always a challenging subject that affects commercial aspects of wastewater treatment plants. The content of nutrients and organic materials in wastewater causes to consider them as a valuable source of energy. The required energy to treat typical wastewater by biochemical reactions and physical separation is in the range of 0.5 to 1 kWhm⁻³ [1], while the internal chemical energy of wastewater is measured between 126 to 280 kWhm⁻³ [2]. So, the energy content of wastewater is more than the required energy for wastewater treatment [3]. Nowadays, wastewater treatment by harnessing the contained energy is shifting from an energy spending problem to a self-sufficient energy resource [2]. The previous research shows that the anaerobic digester and biogas production can gather 0.09-0.14 kWhm⁻³ power [1] which is less than 6% of total energy; therefore the attentions should be focused on other methods to provide energy.

Untreated industrial wastewaters can be a serious threat to water sources because of high pollution; thus, they should be suitably treated [4]. Dye components like methylene blue (MB) in the painting and textile

wastewaters turn them to the toxic and carcinogenic streams [5-7] which biological treatments hardly biodegrade them [5]. On the other hand, some advanced oxidation methods (AOPs) could degrade the organic materials [4-6] and are a proper candidate to use the energy content of wastewater.

Photo Electro Catalysts (PEC) systems degrade organic materials and produce current from anode to cathode electrode. Organic materials like ethanol, methanol, glucose have been used as a sacrificial agent [8, 9]. One of the highest produced power in this method was around 0.567 kW m^{-3} when ethanol was used as a source of carbon [10]. The previous studies showed that using colored organic matters like MB, methyl orange, rhodamine B (RHB) and other disperse dyes from textile industries still produce less photocurrent and power rather than colorless sacrificial agents [9].

However, the performance of PEC is influenced by many parameters like the density of illumination, type, and concentration of sacrificial agents, pH of electrolyte, hydraulic retention time; to the author knowledge, no investigation has been done on the type of membrane in PEC systems. In this study, the performance of PEC is investigated in respect to MB degradation and produced power when Ultra Filtration (UF) and Cation Exchange Membrane (CEM) are used as a separating barrier between anode and cathode chambers.

2. Material and methods

2.1 Experiment description

The performance of using ultra-filtration (UF) and cation exchange membrane (CEM) as a chambers' separator is evaluated by performing a series of photocatalytic experiments in Photo-Electro-Catalytic (PEC) pilot. In this study, methylene blue (MB) was used as a sacrificial agent in anolyte and the MB concentration (mg/l), produced power (μW) between anode and cathode electrodes, the EC ($\mu\text{S/cm}$) and the pH of electrolytes are measured as dependent parameters. Also, the rate of reaction in both UF and CEM case is investigated. Each experiment lasts 24 hrs. The concentration of 1.7 mg/l MB is added to the catholyte in each experiment as a mediator.

2.2 Pilot description

The total volume of the PEC pilot is 1.2 liter that is divided in two equal anode and cathode chambers by Ultra-Filtration (UF) membrane sheet (Sharif Technological Membrane Center, Iran) or CEM (Fuel cell Store, FKB-PK-130, USA) with the active surface of 64 cm^2 (8 cm X 8 cm). By an aquarium air pump (AP-9804, Aqua, China) the catholyte is aerated to supply oxygen for doing reducing reactions. The pilot is shown in Figure 1.

At one side of the anode chamber, a square quartz sheet is set as a window for shining UV light. Each UV lights source (Philips Actinic BL TL, Poland) had a power of 4.5 W and a maximum excitation wavelength of 365 nm. UV lamps and pilot are placed in a dark box to avoid illumination to outside.

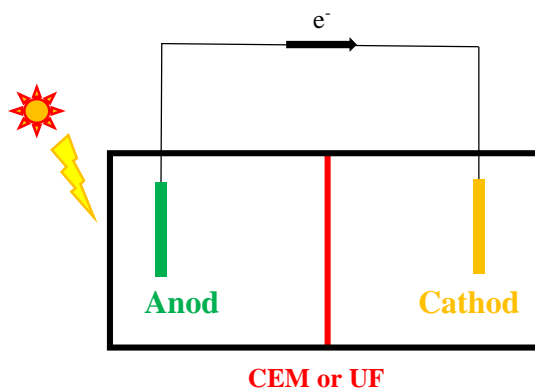


Figure 1. Schematic of PEC pilot.

2.3 Reagents and materials

Analytical grade of acetone ($\text{C}_3\text{H}_6\text{O}$), ammonium fluoride (NH_4F), ethylene glycol ($\text{C}_2\text{H}_6\text{O}_2$), fluoric acid (HF), hydrochloric acid (HCl), hydrogen peroxide (H_2O_2), methanol ($\text{C}_2\text{H}_5\text{OH}$), nitric acid (HNO_3), and sodium hydroxide (NaOH) are used in the experiments (Loba Chemie, India).

2.4 Instruments and measurements

A digital multimeter (UNI-T 139C, Hong Kong) is used to measure the voltage, amperage, and resistance between the anode and cathode. The pH of electrolytes is adjusted with sodium hydroxide and sulfuric acid and is detected by pH meter (Metrohm 691, Swiss), and also the electric conductivity (EC) of the different MB concentrations in electrolytes is measured by EC meter (Inolab cond 7110, Germany). All the measurements are performed in triplicate.

2.5 Fabrication of the Ti/TiO₂-NTA

The commercially pure square Titanium sheet (99.99% purity) of dimensions 10 cm X 10 cm, the thickness of 1 mm, and the active area of 64 cm² is purchased from Sigma-Aldrich and uses as a working electrode. The sample is mechanically polished with different emery type abrasive papers with the grades of 80, 240, 1200, and 2400 before the anodization as proposed by [11] and is rinsed in distilled water. Then the sample is cleaned ultrasonically (Power sonic 420, Hwashin, Korea) in methanol, acetone and deionized water for each 30 min and was washed by distilled water [12]. Finally, it is dried with the oven (BM 120, Fan Aza Gostar, IRAN) at 80 °C for one hr. For chemical etching, the sample is immersed for 1 min in a mixture of HF: HNO₃: H₂O with the volumetric components' ratio of 1:4:5 [11, 13], then is rinsed in acetone and distilled water consequently. The last step of pretreatment is drying with the oven at 70 °C for four hr. [13]. For two-steps electrochemical anodization for the synthesis of TiO₂ nanotube arrays, the process is carried out in an electrolytic cell using the pretreated titanium substrate as an anode. The first step anodization is carried out in electrolyte solution containing 800 ml ethylene glycol, 0.3 wt% (2.67 gr) of NH₄F and 2 wt% (17.81 gr) of distilled water [12]. Anodization is performed at a constant voltage of 30 V [14] using a controlled DC power supply source (Vaxun, PS 302D, China) for 2 hrs. The nanotube layer is removed by sample ultra-sonication first in methanol and then in distilled water each for 20 min. The second step anodization again with the same electrode and electrolyte is carried out by applying 30 V DC electric potential for 8 hrs, then is cleaned with methanol and distilled water for a few minutes. It is annealed at 500 °C for 3 hr with air heating rate of 5 °C/min to enhance the crystallinity of anodic TiO₂ NTs.

2.6 Fabrication of carbon paste electrode

A 10 cm X 10 cm carbon cloth (Avcarb, USA) with Electrical Resistivity of less than 4 mΩ is used as cathode and counter electrode for electrochemical anodization and PEC process. Also 2.5 m platinum wire (Nano-bazar, Iran) with a thickness of 40 μm which is woven throughout all area of it as a catalyst.

3. Results and discussion

3.1 The effects of membrane type on dependent parameters

To investigate the effect of membrane type on PEC's performance, the dependent parameters including MB removal percent in anolyte and catholyte, produced power and pH changes are investigated when CEM and UF membrane are used as separator membranes. During this experiment, the initial MB's concentration of anolyte, catholyte, and the density of illumination are 17 mg/l, 1.7 mg/l, and 8 W, respectively at the start of the experiment. The amount of pH in anolyte and catholyte are neutral at the start of each step. 1.7g salt is added to catholyte in each step to increase the electrical conductivity.

3.1.1 MB concentration of anolyte and catholyte and produced power

The results show that the MB removal percent in anolyte in the case of UF membrane is more than CEM, while the MB removal percent in catholyte and produced power are more when CEM is used (Figure 2). The maximum produced power in the case of CEM is 0.899 μW while in the case of UF, it is 1.016 μW.



CEM only allows cations to move from anolyte to catholyte and prevents the anions from transferring, so it causes the flux of H⁺ that is produced during the anodic half-reaction (equation 1) be higher in comparison with the UF membrane. Therefore, it could be concluded in the case of CEM, the concentration of proton be more in catholyte. Since, H⁺ is one of the reactants in cathodic half-reaction (equation 2), the rate of cathodic half-reaction in CEM case was more than that of in the UF membrane. As a result, the density of current and produced power in CEM are more in comparison with the UF membrane. Moreover,

water is one of the products of the cathodic half-reaction, so higher in the rate of cathodic half-reaction causes more dilution is occurred and then increases the MB removal percent in catholyte in the case of CEM.

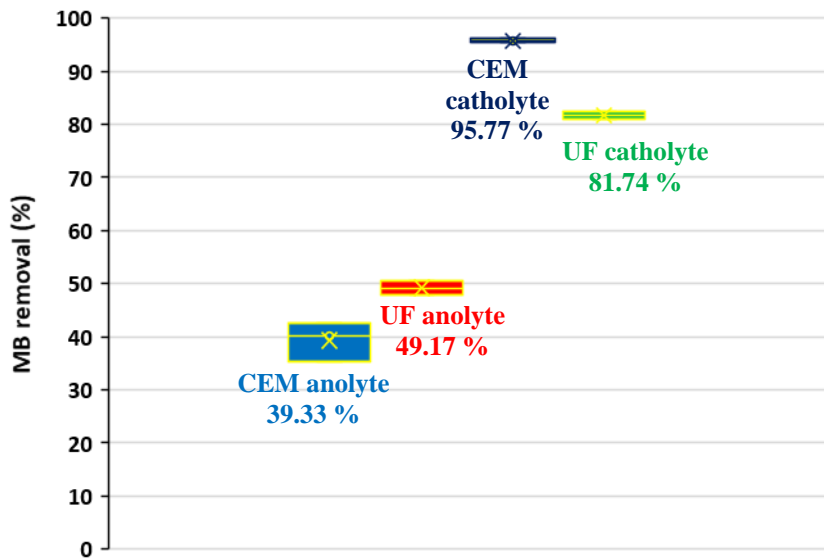


Figure 2. MB removal percent in anolyte and catholyte when UF and CEM are used.

The concentration of MB in anolyte can be decreased in two ways. One is due to the oxidation reaction (equation 1) and second is due to dilution. The prior way is common in both CEM and UF membrane, while the last one only is occurred in the UF membrane because hydroxide can freely move toward anolyte from catholyte to produce water. The high concentration of H^+ in anolyte attracts OH^- which is produced through reduction reaction in catholyte, so as it is expected, the MB removal percent of anolyte in UF case is more than that of CEM one.

3.1.2 PH

The pH changes at the mentioned condition showed when UF membrane is used, the pH in anolyte and catholyte decreases and increases respectively. H^+ is produced in the anolyte during anodic half-reaction so decreases the pH value, while OH^- is produced in the catholyte during cathodic half-reaction so increases the pH value. However, in the case of CEM, the trends are reversed (Figure 3). The CEM only allows H^+ to transfer easily from anolyte to catholyte, so the concentration of H^+ decreases in anolyte and the amount of pH rises. On the other hand, the transferred H^+ neutralizes the produced OH^- in catholyte, so the amount of pH drops in catholyte. These phenomena confirm the high concentration of H^+ and the great attraction of OH^- in anolyte in the case of UF membrane.

3.2 The impact of EC of catholyte on dependent parameters

The EC of catholyte can affect the performance of PEC [15], therefore the different concentrations of salt were added to catholyte when UF and CEM are used as membrane and the MB removal percent in anolyte and produced power are analyzed. The initial amount of MB concentration in anolyte, catholyte, and the density of illumination are similar to the previous experiment else catholyte salt concentration that is changed in each step.

The salt concentration in catholyte has a direct relation with MB removal percent in anolyte until a particular salt concentration, and after that, the MB removal percent remains stable. The optimum point for UF membrane is 10 g/l, and that of for CEM is 5 g/l, which is pointed in Figure 4.

This finding shows the direct relation between the salt concentration of catholyte and MB removal percent in anolyte continues in higher salt concentrations in the case of UF in comparison with CEM. Moreover, the salt concentration in catholyte has more effect on MB removal percent in anolyte in the UF membrane comparing with CEM. The most MB removal percent in anolyte is 98.51% in the case of UF, while that of is 52.01% in the case of CEM after 24 hr.

In the UF membrane, both cations and anions in the catholyte could transfer to anolyte, while in the CEM only cations are allowed to move, so adding salt in catholyte causes more ion movement from catholyte to anolyte in the UF case rather than CEM. This increases in ions movement augment the conductivity in electrolytes, which finally increases MB removal percent in the UF case in a higher value.

The produced power trend in different salt concentration of catholyte for both CEM and UF is shown in Figure 5.

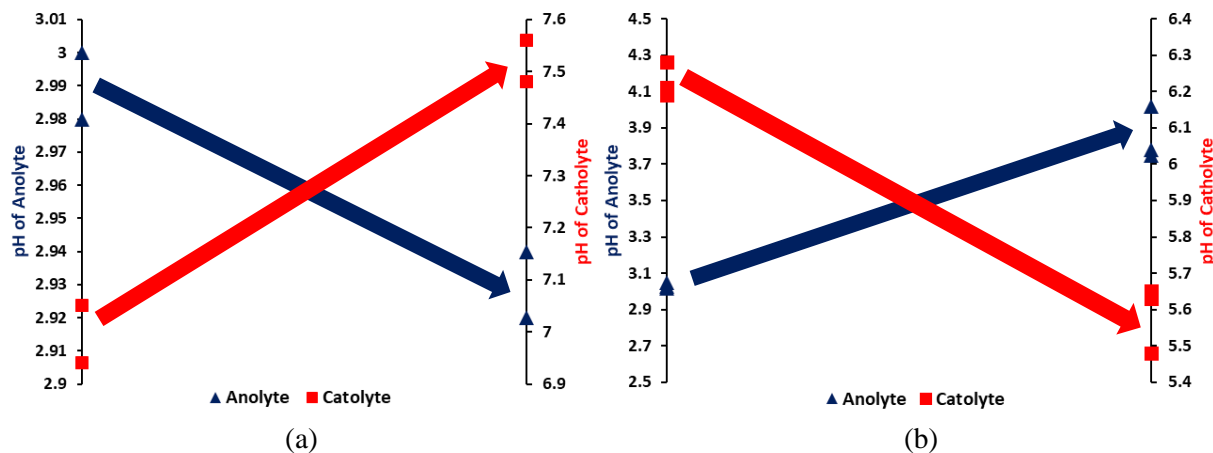


Figure 3. The pH changes in anolyte and catholyte when (a) UF and (b) CEM were used.

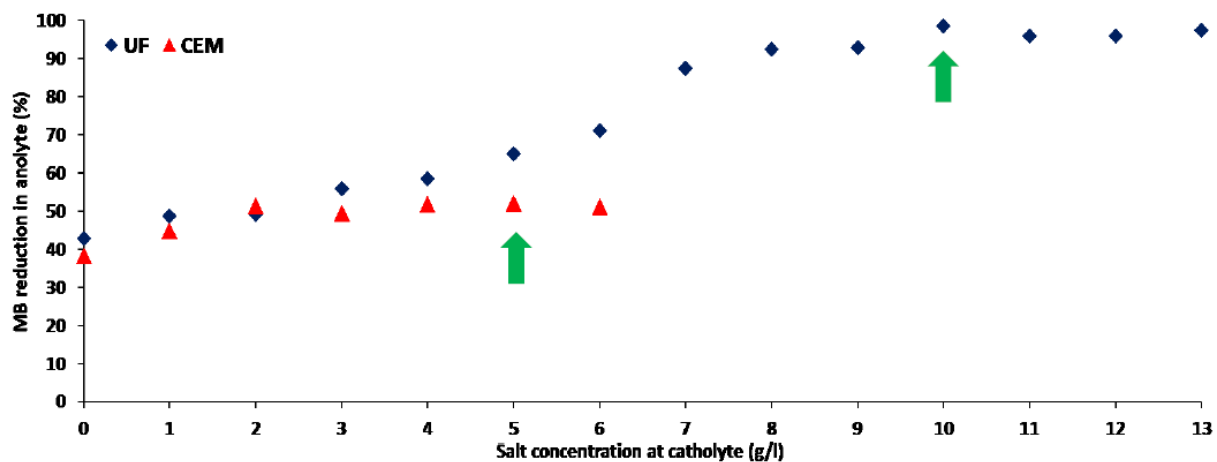


Figure 4. The effect of the salt concentration of catholyte on MB removal percent in anolyte.

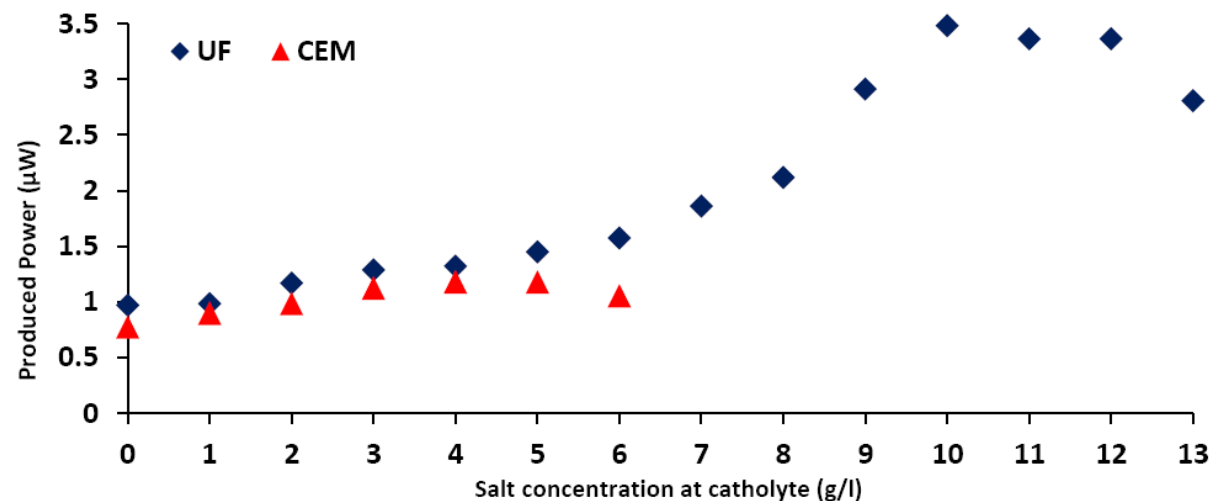


Figure 5. The effect of the salt concentration of catholyte on produced power.

Increase in EC of catholyte produces more power both in CEM and UF membrane, while its effect on UF membrane is more and prolonged rather than CEM. However, at high salt concentration, more than 10 and 4 g/l for UF and CEM case, respectively, decrease trends in produced power are observed. It is inferring when the salt concentration be high enough, a disturbance in ions movement has occurred that has a negative effect on produced power.

3.3 UV-visible test of MB

To investigate the degradation of MB concerning time, the UV-visible reflectance spectra versus wavelength in different time intervals is done in the wavelength range from 450 to 700 nm when UF and CEM are used. In this experiment, the density of illumination is 8 W, and the MB concentration of anolyte and catholyte are 17 and 1.7 mg/l, respectively. The salt concentration of catholyte is set 5 and 10 g/l for CEM and UF membrane, respectively, because based on the previous experiment, the performance of the system has the maximum amounts.

As the Figure 6 shows, the maximum absorbance and peak value at 665 nm at the first of experiment, decreases gradually concerning time, so it proofs the concentration of MB decreases moderately with exposure to time due to photo-electro-catalytic oxidation of MB in both UF and CEM cases. In UF case, the absorbance peak turns to nearly smooth, and blue color of solutions became colorless with passing time; this visually confirms the reaction solution de-coloration. As MB is degraded, the absorbance peaks are shifted with irradiation time, which shows the formation of byproducts during the degradation process. Similar results are found in previous studies [4, 6, 14, 16].

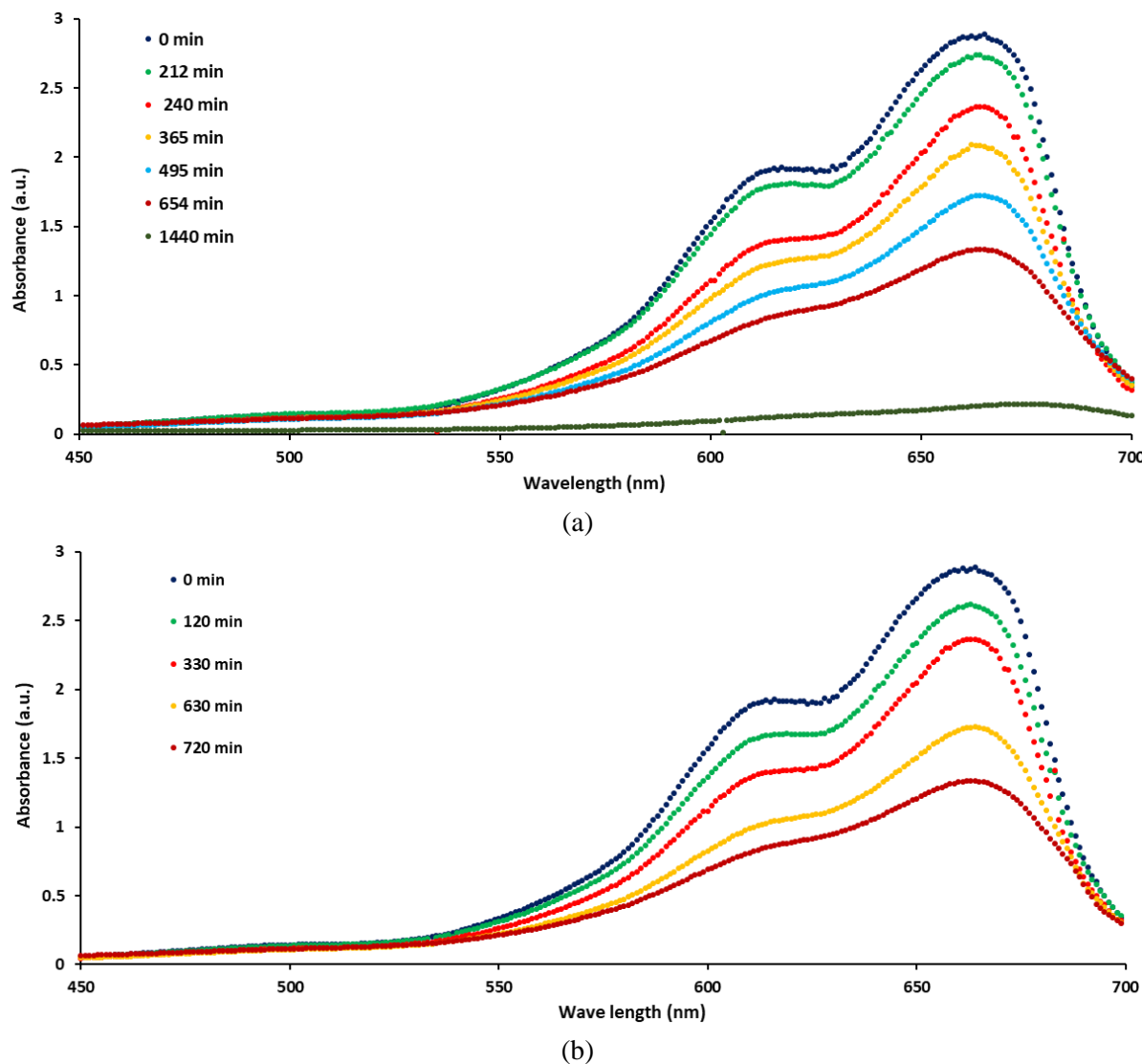


Figure 6. Spectral changes of MB spectra versus wavelength under a) UF membrane b) CEM mood.

3.4 The kinetic of reaction

To investigate the photocatalytic degradation profiles of MB, six kinetic models are applied based on previous studies [6, 13, 14, 16, 17] including zero-order, half order, first order, second order, parabolic diffusion, and the modified Freundlich model. The parabolic diffusion model explains the diffusion-controlled photocatalytic degradation and modified Freundlich model elucidates the experimental data on molecular ion exchange and diffusion-controlled process [16]; In fact, this model describes heterogeneous diffusion from the flat surfaces by molecular ion exchange [16]. The initial condition for this step was similar to the previous one.

$$C - C_0 = -kt \quad (\text{Zero order})$$

$$\sqrt{C} - \sqrt{C_0} = -kt \quad (\text{half order})$$

$$\ln \left(\frac{C}{C_0} \right) = -kt \quad (\text{First order})$$

$$\frac{1}{C_0} - \frac{1}{C} = -kt \quad (\text{Second order})$$

$$\frac{(1 - \frac{C}{C_0})}{t} = kt^{-0.5} + a \quad (\text{Parabolic diffusion model})$$

$$\ln \left(1 - \frac{C}{C_0} \right) = \ln(k) + b \ln(t) \quad (\text{Freundlich model})$$

In the above equations, C_0 and C are the concentration of MB at irradiation time 0 and t , respectively, and k is the corresponding rate constant.

3.4.1 MB versus time

The MB removal percent in anolyte by nanostructured TiO₂ films under UV-visible irradiation in a different time is drawn to investigate its trend when UF and CEM are used. As Figure 7 shows, MB removal percent has an ascending trend, and after approximately 1310 min for UF membrane and 1080 min for CEM, the removal percent be stable. Finally, 93.70% and 52.03% of MB in anolyte in UF and CEM cases, respectively, are degraded after 1440 minutes.

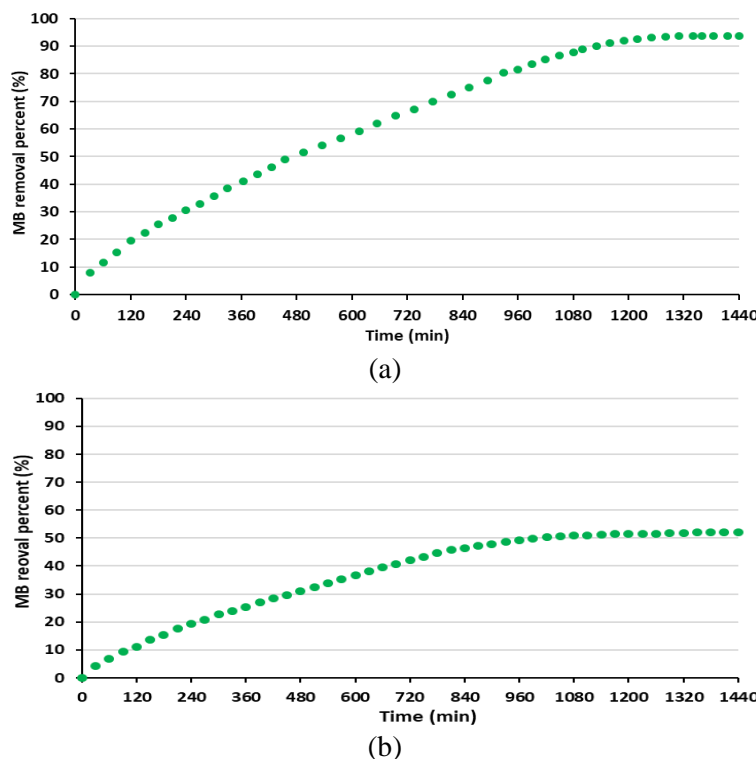


Figure 7. The MB removal percent of anolyte vs time in a) UF case and b) CEM case.

3.4.2 The kinetics models

Six models are applied to explore the mechanisms of adsorption and kinetic behavior of photo-electro-catalytic degradation processes by nanostructured TiO_2 films at room temperature (Figures 8 and 9). The corresponding linear correlation coefficient (R^2) and photo-electro-catalytic degradation rate constant (K) are calculated, and in order to perform good comparison are shown in Table 1 for both UF membrane and CEM cases.

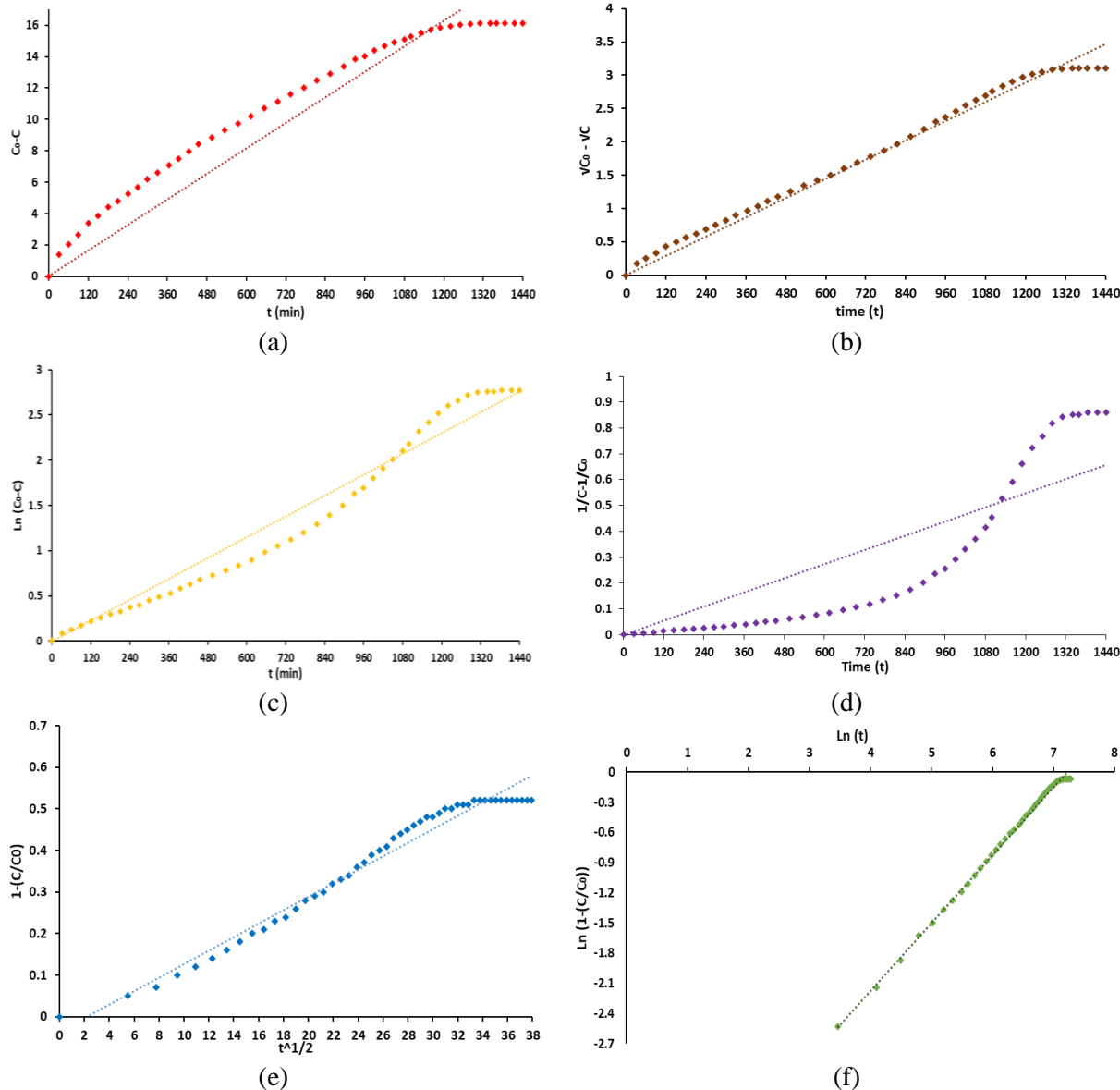


Figure 8. Photocatalytic degradation kinetics of the four models of MB in UF mood. (a) zero-order, (b) half-order, (c) first-order, (d) second-order, (e) parabolic diffusion, and (f) modified Freundlich models.

The dotted lines show linear fitting of the corresponding models.

Table 1. R^2 and K values in UF membrane and CEM cases' kinetics models.

Kinetic model	UF membrane		CEM	
	R^2	K	R^2	K
Zero-order model	0.75	0.0078	0.75	0.0078
Half-order	0.98	0.0024	0.83	0.0011
First-order model	0.88	0.0006	0.88	0.0006
Second-order	0.74	0.0005	0.95	0.00005
Parabolic diffusion model	0.97	0.016	0.97	0.0162
Modified Freundlich model	0.99	0.00772	0.99	0.005052

The experimental data are analyzed with the six mentioned kinetic models. It is evident from the Figure 8 shows that the experimental data do not fit well to the zero, first and second-order models; while the kinetics of adsorption and photo electrocatalytic degradation can be predicted more accurately by the half order, modified Freundlich and parabolic diffusion models for UF membrane case. This finding shows the concentration of MB influences on MB degradation in some order of magnitude.

In the case of CEM, the second-order modified Freundlich, and parabolic diffusion models fit well to experimental data, while zero-order, half, and first-order models could not predict the data accurately (Figure 9). During MB degradation, it is finally converted to carbon dioxide and water according to equation 3.



By comparison, the R^2 of different kinetic models in UF and CEM case is found that the photocatalytic degradation of MB in the case of CEM follows the second-order model, while that of UF membrane half-order model. This result indicates that the concentration of MB in the case of CEM plays a more important role in the kinetics of reaction rather than UF membrane.

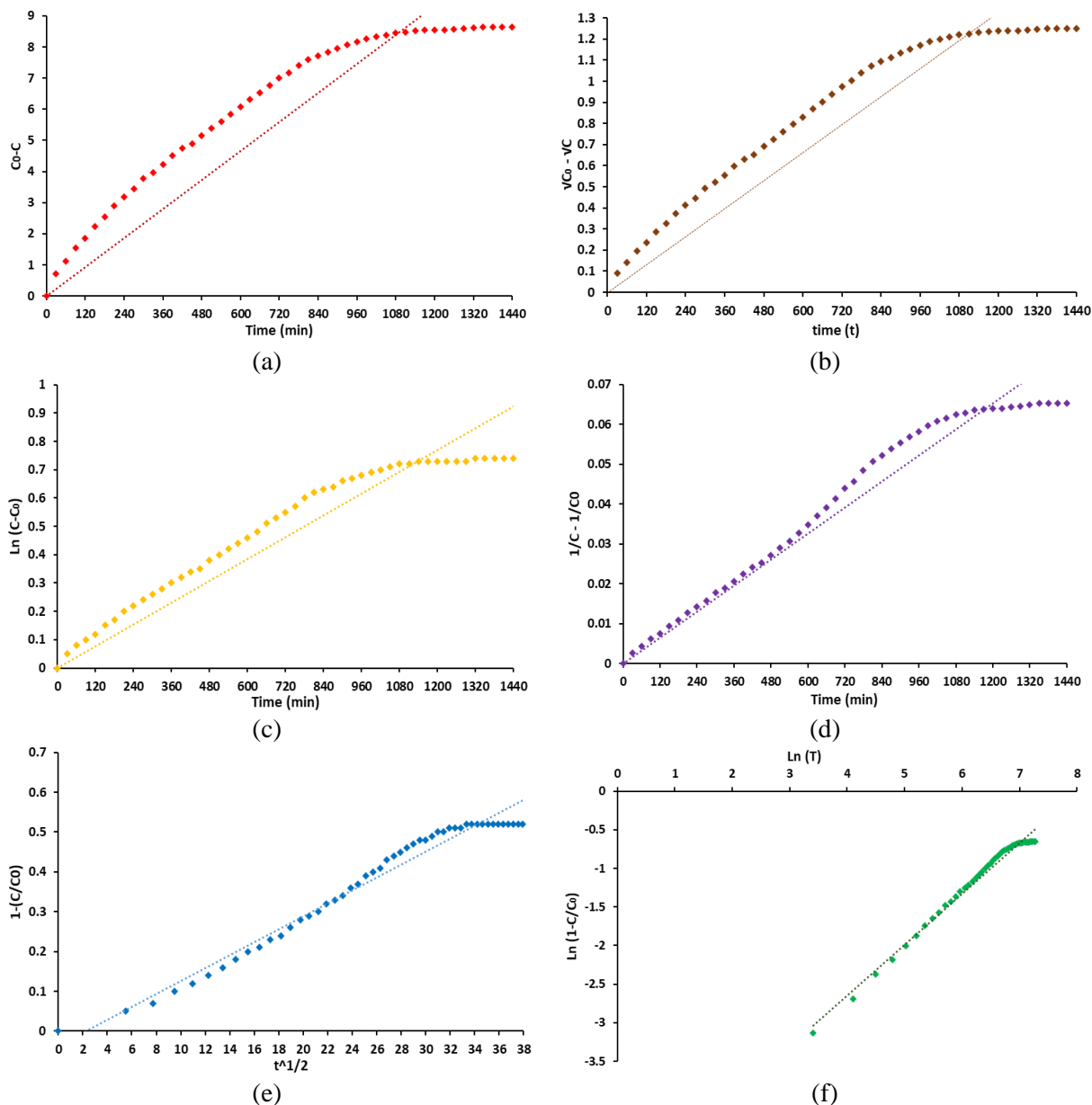


Figure 9. Photocatalytic degradation kinetics of the four models of MB in CEM mood. (a) zero-order, (b) half-order, (c) first-order, (d) second-order, (e) parabolic diffusion, and (f) modified Freundlich models of methylene blue. The dotted lines show linear fitting of the corresponding models.

4. Conclusion

The performance of the photo-electro-catalytic system on MB degradation and production of power are investigated when CEM and UF membrane are used as an anode and cathode chamber separators. In the same condition, MB removal percent in anolyte is more in UF case, while the produced power is higher in CEM case. Increasing in the salt concentration in the catholyte can increase the MB removal percent and produced power until an optimum point both in CEM and UF, while its effect on UF is in a higher amount. Moreover, the EC and pH changes in anolyte and catholyte chambers are investigated. Six kinetic models are applied to experimental data for both CEM and UF membrane, which show for the UF membrane half-order model and for CEM, second-order model could predict well the data. So the concentration of MB has more impact on MB removal percent in CEM rather UF membrane. Moreover, both parabolic diffusion and the modified Freundlich model could fit the data both in the CEM and UF membrane.

Acknowledgment

This work was funded by Hormozgan water and Wastewater Company

References

- [1] B. Kokabian and V. G. Gude, "Photosynthetic microbial desalination cells (PMDCs) for clean energy, water and biomass production," *Environmental Monitoring*, vol.15, p.2178-2185, 30 September 2013.
- [2] E. Heidrich, T. Curtis and J. Dolfing, "Determination of the Internal Chemical Energy of Wastewater," *Environmental Science & Technology*, vol. 45, p. 827-832, January 2011.
- [3] B. E. Logan and K. Rabaey, "Conversion of Wastes into Bioelectricity and Chemicals by Using Microbial Electrochemical Technologies," *Science*, vol. 337, p. 686, 2012.
- [4] R. Dariania, A. Esmaeili, A. Mortezaali, S. Dehghanpour, "Photocatalytic reaction and degradation of methylene blue on TiO₂ nano-sized particles," *Optik*, vol.127, no.7, pp.143-7154, 2016.
- [5] N. Yuangpho, D. T. T. Trinh, D. Channei, W. Khanitchaidecha and A. Nakaruk, "The influence of experimental conditions on photocatalytic degradation of methylene blue using titanium dioxide particle," *the Australian Ceramic Society*, vol. 54, pp. 557-564, 28 March 2018.
- [6] Y. m. Hunge, "Photoelectrocatalytic Degradation of Methylene Blue using Spray Deposited Zno Thin Films under UV Illumination," *MOJ Polymer Science*, vol. 1, no. 4, 2017.
- [7] Q. Zhao, Z. Li, Q. Deng, L. Zhu, S. Luo, H. Li, "Paired photoelectrocatalytic reactions of glucose driven by a photoelectrochemical fuel cell with assistance of methylene blue," *Electrochimica Acta*, 2016.
- [8] B. G. Garcia, T. T. Guaraldo, J. F. d. Brito, M. F. Brugnera, M. V. B. Zanoni, "Achievements and Trends in Photoelectrocatalysis: from Environmental to Energy Applications," *Electrocatalysis*, pp.1-27, 2015.
- [9] P. Lianos, "Review of recent trends in photoelectrocatalytic conversion of solar energy to electricity and hydrogen," *Applied Catalysis B: Environmental*, vol. 210, p. 235-254, 2017.
- [10] S. Sfaelou, L. Sygellou, V. Dracopoulos and A. Travlos, "Effect of the Nature of Cadmium Salts on the Effectiveness of CdS SILAR Deposition and Its Consequences on the Performance of Sensitized Solar Cells," *Physical Chemistry*, vol. 118, p. 22873-22880, 16 September 2014.
- [11] M. M. Momeni, M. M. Momeni and M. Davarzadeh, "Single-step electrochemical anodization for synthesis of hierarchical WO₃-TiO₂ nanotube arrays on titanium foil as a good photoanode for water splitting with visible light," *Electroanalytical Chemistry*, vol. 739, pp. 149-155, 30 December 2015.
- [12] N. Pishkar, M. Ghoranneviss, Z. Ghorannevis, H. Akbari, "Study of the highly ordered TiO₂ nanotubes physical properties prepared with two-step anodization," *Physics*, vol.9, pp.1246-1249, 2018.
- [13] M. T.-H. Liu, J. Zhang and B. Wang, "Fabrication of Titanium dioxide nanotube photo-electrodes in different electrolyte mixtures and the impacts on their characteristics and photo-catalytic abilities under visible light," *Chemical Technology*, vol. 19, no. 1, pp. 34-40, 2017.
- [14] M. Yurddaskal, T. Dikici, S. Yildirim, M. Yurddaskal, M. Toparli and E. Celik, "Fabrication and characterization of nanostructured anatase TiO₂ films prepared by electrochemical anodization and their photocatalytic properties," *Alloys and Compounds*, 2015.
- [15] T. Fang, C. Yang and L. Liao, "Photoelectrocatalytic degradation of high COD dipterex pesticide by using TiO₂/Ni photo electrode," *Environmental Sciences*, vol. 24, no. 6, pp. 1149-1156, 2012.
- [16] M. J. Uddin, M. A. Islam, M. A. Islam, S. Hasan, M. S. A. Amin and M. M. Rahman, "Preparation of nanostructured TiO₂-based photocatalyst by controlling the calcining temperature and pH," *International Nano Letters*, pp. 2-19, 2012.
- [17] X. Lv, H. Zhang and H. Chang, "Improved photocatalytic activity of highly ordered TiO₂ nanowire arrays for methylene blue degradation," *Materials Chemistry and Physics*, vol.138, p.789-795, 2012.

Seyed Ali Rahmaninezhad: rahmaninezhad@ut.ac.ir, ali.rahmaninezhad@gmail.com